

Unusual Structural, Functional, and Stability Properties of Serine Hydroxymethyltransferase from *Mycobacterium tuberculosis**

Received for publication, June 12, 2003, and in revised form, July 28, 2003
Published, JBC Papers in Press, August 11, 2003, DOI 10.1074/jbc.M306192200

Sarita Chaturvedi and Vinod Bhakuni‡

From the Division of Molecular and Structural Biology, Central Drug Research Institute, Lucknow 226 001, India

From the genome analysis of the *Mycobacterium tuberculosis* two putative genes namely *GlyA* and *GlyA2* have been proposed to encode for the enzyme serine hydroxymethyltransferase. We have cloned, overexpressed, and purified to homogeneity their respective protein products, serine hydroxymethyltransferase, SHM1 and SHM2. The recombinant SHM1 and SHM2 exist as homodimers of molecular mass about 90 kDa under physiological conditions, however, SHM2 has more compact conformation and higher thermal stability than SHM1. The most interesting structural observation was that the SHM1 contains 1 mol of pyridoxal 5'-phosphate (PLP)/mol of enzyme dimer. This is the first report of such a unique stoichiometry of PLP and enzyme dimer for SHMT. The SHM2 contains 2 mol of PLP/mol of enzyme dimer, which is the usual stoichiometry reported for SHMT. Functionally both the recombinant enzymes showed catalysis of reversible interconversion of serine and glycine and aldol cleavage of a 3-hydroxyamino acid. However, unlike SHMT from other sources both SHM1 and SHM2 do not undergo half-transamination reaction with D-alanine resulting in formation of apoenzyme but L-cysteine removed the prosthetic group, PLP, from both the recombinant enzymes leaving the respective inactive apoenzymes. Comparative structural studies on the two enzymes showed that the SHM1 is resistant to alkaline denaturation up to pH 10.5, whereas the native SHM2 dimer dissociates into monomer at pH 9. Urea- and guanidinium chloride-induced two-step unfolding of SHM1 and SHM2 with the first step being dissociation of dimer into apomonomer at low denaturant concentrations followed by unfolding of the stabilized monomer at higher denaturant concentrations.

Recent years have seen increased incidence of tuberculosis in both developing and developed countries. Information available from the complete genome sequence of *Mycobacterium tuberculosis* has the potential of providing the information that would generate knowledge that will enable to elucidate the unusual biology of its etiological agent, *M. tuberculosis*.

Serine hydroxymethyltransferase (SHMT),¹ L-serine:tetra-

hydrofolate 5,10-hydroxymethyltransferase is a pyridoxyl 5'-phosphate (PLP)-dependent enzyme. SHMT reaction plays a major role in cell physiology as it is considered to be a key enzyme in the pathway for interconversion of folate coenzymes that provide almost exclusively one-carbon fragments for the biosynthesis of a variety of end products such as DNA, RNA, ubiquinone, methionine, etc. (1–3). The physiological role of SHMT is the reversible interconversion of serine to glycine and irreversible hydrolysis of 5,10-CH⁺-H₄PteGlu to 5-CHO-H₄PteGlu. In addition to these physiological reactions, SHMT also catalyzes, in the absence of H₄PteGlu, the retroaldol cleavage of several 3-hydroxyamino acids, such as *allo*-threonine, and the transamination and slow racemization of D- and L-alanine (4, 5).

SHMT shows a ubiquitous distribution in nature, being found both in the prokaryotes and eukaryotes. In eukaryotes, SHMT exists as both cytosolic and mitochondrial isoforms (6) encoded by the separate genes (7). A chloroplast isoform has also been reported to be present in the plants (8) and *Euglena gracilis* (9). Three molecular forms of SHMT have been detected in choanoflagellates of *Crithidia fasciculata*. One of them is cytosolic, whereas the other two forms are particle bound, one being mitochondrial and the other one very likely is glycosomal (10). A single form of SHMT has been detected in epimastigotes of *Trypanosoma cruzi* (11).

Structurally SHMT from a mammalian source is a homotetramer with a subunit molecular mass of about 53 kDa and contains 4 mol of PLP/mol of enzyme (12, 13). The structural details have revealed that the tetrameric enzyme is a dimer of dimers (13). The three SHMT isoforms found in *C. fasciculata* also have tetrameric structure (10). In contrast, the SHMT from *Escherichia coli* as well as from several other bacterial sources are dimeric and contain 2 mol of PLP/mol of enzyme (14). Recently, it has been shown that the *T. cruzi* SHMT is present as a catalytically active monomer (11). X-ray crystal structure has shown that the coenzyme PLP is covalently attached to the enzyme molecule and is located at the dimer interface (12–14).

The folding/unfolding of both the tetrameric and the dimeric SHMTs have been extensively studied (15–18). The tetrameric SHMT undergoes a reversible unfolding with the first step being dissociation of tetramer into dimer accompanied by the removal of the enzyme-bound PLP from the active site (15). Regarding the second step it was not clear whether the stabilized dimer of SHMT unfolds directly or does so via the formation of monomer (15). For the dimeric SHMTs, both from *E. coli* and *Bacillus subtilis*, the first step of unfolding is dissociation of the native dimer into monomer followed by the unfolding of

* This work was supported by grants from the National Bioscience Award for Career Development from the Department of Biotechnology, New Delhi, and Indian Council of Medical Research Grant SSP150 (to V. B.) and the Council of Scientific and Industrial Research, New Delhi (to S. C.). The costs of publication of this article were defrayed in part by the payment of page charges. This article must therefore be hereby marked "advertisement" in accordance with 18 U.S.C. Section 1734 solely to indicate this fact.

‡ To whom correspondence should be addressed: Division of Molecular and Structural Biology, Central Drug Research Institute, Lucknow 226 001, India. Fax: 91-522-223405; E-mail: bhakuni@rediffmail.com.

¹ The abbreviations used are: SHMT, serine hydroxymethyltrans-

ferase; PLP, pyridoxal 5'-phosphate; H₄PteGlu, N⁵-formyl-5,6,7,8-tetrahydropteroyl-L-glutamic acid; DTT, dithiothreitol; *T_m*, midpoint of thermal denaturation; GdmCl, guanidinium chloride; PyP, pyridoxamine-P; FRET, fluorescence resonance energy transfer.

the stabilized monomer (16–18). However, for the thermophilic SHMT from *Bacillus stearothermophilis*, a highly cooperative unfolding of the native dimer into unfolded monomer was reported (18).

Searches of the *M. tuberculosis* genome for enzymes related to SHMT have lead to the identification of two genes namely the *GlyA* and *GlyA2*, which have been proposed as putative genes encoding for SHMTs in the organism. Here we report the cloning, overexpression, and purification of the recombinant SHM1 and SHM2, the protein products of the genes *GlyA* and *GlyA2*. Furthermore, the structural, functional, and stability properties as well as the comparative studies on thermal, pH-, urea-, and GdmCl- induced unfolding of both recombinant proteins have been discussed in detail.

EXPERIMENTAL PROCEDURES

Cloning, Overexpression, and Purification of the Proteins of *M. tuberculosis GlyA* and *GlyA2* Genes—The complete genes of *M. tuberculosis* encoding functional *GlyA* and *GlyA2* were amplified separately by PCR from the genomic DNA. The different oligonucleotides used for *GlyA*, based on the reported gene sequence (GenBank™ accession number Rv1093), were upstream 5'-GGAATTCCATATGCTGCCCGCTCGC-TGAAGTT-3' and downstream 5'-CCCAAGCTTGCGGCCGACCAGAC-TCCACTC-3' for histidine-tagged protein and 5'-CCCAAGCTTTAG-CGGCCGACCAGACTCCACTC-3' for non-histidine-tagged protein. The different oligonucleotides for *GlyA2* (GenBank™ accession number Rv0070c) were upstream 5'-GGAATTCCATATGAACACCTCAACGACTCCCTG-3' and downstream 5'-ATAAGAATGCGGCCGCTGTACGATGTCAGTTCCGGGTA-3' for histidine-tagged protein and 5'-CCCAAGCTTTTATGTACGATGTCAGTTCCGTA-3' for non-histidine-tagged protein. Reactions were carried out in two phases for 5 and 30 cycles in a total volume of 50 μ l with 2.5 units of *Taq* polymerase. For *GlyA*, the first cycle without overhang amplification was 95 °C, 1 min; 54 °C, 1 min; 72 °C, 2 min; and the second cycle with overhang amplification was 95 °C, 1 min; 60 °C, 1 min; 72 °C, 2 min with final extension for 10 min. For *GlyA2*, the first cycle without overhang amplification was 95 °C, 1 min; 44 °C, 1 min; 72 °C, 2 min, and the second cycle was similar to the first cycle except for the annealing temperature of 56 °C with final extension for 10 min. The amplified product was cloned into pET-22b between the *NdeI* and *HindIII* sites. DNA sequencing confirmed the homogeneity of the sequences. The resultant constructs were transformed into C41(DE3).

A single colony was inoculated into 10 ml of 2 \times YT broth having ampicillin at a concentration of 100 μ g/ml and grown overnight at 30 °C. It was then subcultured in 1 liter of 2 \times YT media containing similar ampicillin concentrations. For SHM1, the culture was induced with 0.5 mM isopropyl-1-thio- β -D-galactopyranoside at A_{600} of 0.4 to 0.5 for 12 h at 30 °C, whereas SHM2 was grown for 18 h without any induction. The cell culture was harvested followed by suspension into 50 mM potassium phosphate buffer, pH 7.8, containing 400 mM NaCl, 10 mM imidazole, 1 mM β -mercaptoethanol, and 50 μ M PLP. Cells were sonicated and centrifuged to remove the cell debris. The supernatant was loaded on a nickel-nitrilotriacetic acid-agarose column pre-equilibrated with the same buffer. To remove the nonspecific binding protein constituents, the column was washed with 50 mM potassium phosphate buffer, pH 7.4, containing 400 mM NaCl and 80 mM imidazole. The protein was eluted with the same buffer containing 300 mM imidazole. The fractions containing SHMT were pooled and glycerol and DTT were added to final concentrations of 8% and 1 mM, respectively. Excess imidazole was removed by dialysis against 25 mM potassium phosphate buffer, pH 7.6, containing 50 mM NaCl, 1 mM EDTA, 8% glycerol, and 1 mM DTT. The purity of the purified proteins was checked by SDS-PAGE (19) and ESI-MS and was found to be about 99% pure.

Circular Dichroism Measurements—The CD measurements were made with a Jasco J810 spectropolarimeter calibrated with ammonium (+)-10-camphorsulfonate and the results were expressed as relative ellipticity and plotted as percentage values. The CD spectra were obtained at enzyme concentrations of 2 and 10 μ M for far-UV CD and visible CD measurements, respectively, with a 2-mm cell at 4 °C. The values obtained were normalized by subtracting the baseline recorded for the buffer having the same concentration of denaturant under similar conditions.

Synthesis of PyP-SHMT—The reduction of the PLP aldimine was achieved according to the procedure of Cai and Schirch (20).

Enzyme Activity—SHMT activity of the purified recombinant pro-

teins were determined as reported earlier (21, 22). Briefly, a 0.1-ml reaction mixture contained 400 mM potassium phosphate buffer, pH 7.6, 1.8 mM DTT, 1 mM EDTA, 50 μ M PLP, 1.8 mM tetrahydrofolate, 3.6 mM L-[3- 14 C]serine, and approximately 1 μ M protein. After incubation at 37 °C for 20 min the reaction was stopped by the addition of 100 μ l of dimedone (400 mM in 50% ethanol). The reaction mixture was kept in boiling water bath for 5 min and the H- 14 CHO-dimedone adduct was extracted into 3 ml of toluene. A 1-ml volume of toluene extract was added to 5 ml of scintillation fluid (0.6% (w/v) 2,5-diphenyloxazole) and the radioactivity was measured on the scintillation counter.

Activity was also measured by another reported method (23). A 1-ml reaction mixture contained 1–70 μ g of enzyme, alcohol dehydrogenase (100 μ g), NADH (250 μ M), 10 mM *allo*-threonine in 25 mM potassium phosphate buffer, pH 7.6, 1 mM EDTA, and 1 mM DTT. The reference cuvette contained all the chemicals except *L*-*allo*-threonine. The activity was observed as decrease in the absorbance at 340 nm. The NADH consumed in the reaction was calculated using a molar extinction coefficient of 6220 M $^{-1}$ cm $^{-1}$.

Fluorescence Measurements—Fluorescence spectra were recorded with PerkinElmer LS5B spectroluminescencemeter in a quartz cell with a 5-mm path length. All samples were incubated for 6 h under specified conditions before recording the spectra. For tryptophan fluorescence measurements the excitation wavelength was 290 nm and the spectra were recorded from 300 to 400 nm. The protein concentration used was 2 μ M and the measurement was carried out at 25 °C. For FRET studies the samples were excited at 290 nm and the spectra were recorded from 300 to 450 nm.

Cross-linking Using Glutaraldehyde—To the native and urea- or GdmCl-treated SHMT (1 μ M enzyme), an aliquot of 25% (w/v) glutaraldehyde was added to obtain a final glutaraldehyde concentration of 1%. The samples were incubated at 25 °C for 5 min followed by quenching of the cross-linking reaction by the addition of 200 mM sodium borohydride. After incubation for 20 min, 3 μ l of 10% aqueous sodium deoxycholate was added. The pH of the reaction mixtures was lowered to 2–2.5 by the addition of orthophosphoric acid, which resulted in precipitation of the cross-linked proteins. After centrifugation (13,000 \times g, 4 °C, 10 min) the obtained precipitates were re-dissolved in 0.1 M potassium phosphate buffer, pH 7.6, 1% SDS, and 50 mM DTT and heated at 90–100 °C for 5 min. The molecular mass of the cross-linked products was determined by 10% SDS-PAGE (19).

Size Exclusion Chromatography—The gel filtration experiments were carried out on a Superdex 200HR 10/30 column (manufacturer's exclusion limit 600 kDa for proteins) on AKTA FPLC (Amersham Biosciences). The columns were equilibrated and run on 25 mM potassium phosphate buffer, pH 7.6, containing 1 mM EDTA, 100 mM NaCl, and 2 mM β -mercaptoethanol (or mentioned otherwise) and the desired urea or GdmCl concentration at 4 °C. The SHMT solution (10 μ M) was incubated at the desired GdmCl or urea concentrations for 6 h at 4 °C. These samples (200 μ l) were loaded on the column and run at 4 °C with a flow rate of 0.3 ml/min.

pH-dependent Incubation—Recombinant SHM1 and SHM2 were dissolved in 10 mM citrate/glycine/Hepes buffer (pH of the solution maintained) of desired pH values and incubated for 4 h at 4 °C before making the measurements.

Urea or Guanidinium Chloride Denaturation of SHMT—Recombinant SHM1 and SHM2 (2 μ M) were dissolved in 25 mM potassium phosphate buffer, pH 7.6, containing 1 mM EDTA, 50 mM NaCl, and 1 mM DTT in the presence and absence of increasing concentrations of urea or GdmCl and incubated for 6 h at 4 °C. These samples were then used for taking various measurements.

RESULTS AND DISCUSSION

Expression and Purification

The expression of both the SHM1 and SHM2 was good and the expressed proteins were present predominantly (>90%) in the soluble fraction. The enzymes present in the soluble fraction were purified by the method described under "Experimental Procedures." The yield of both the enzymes was in the range of 12 to 15 mg/liter. The purified proteins were homogenous as indicated by a single protein band on SDS-PAGE (Fig. 1, A and B) and a single peak in ESI-MS (data not shown). The purified enzymes were assayed for SHMT activity (21, 22) and the specific activity of 1.2 ± 0.2 and 1.8 ± 0.3 units/mg was observed for the SHM1 and SHM2, respectively. The 280/425 absorbance ratio was 4.78 and 3.43 for the purified recombi-

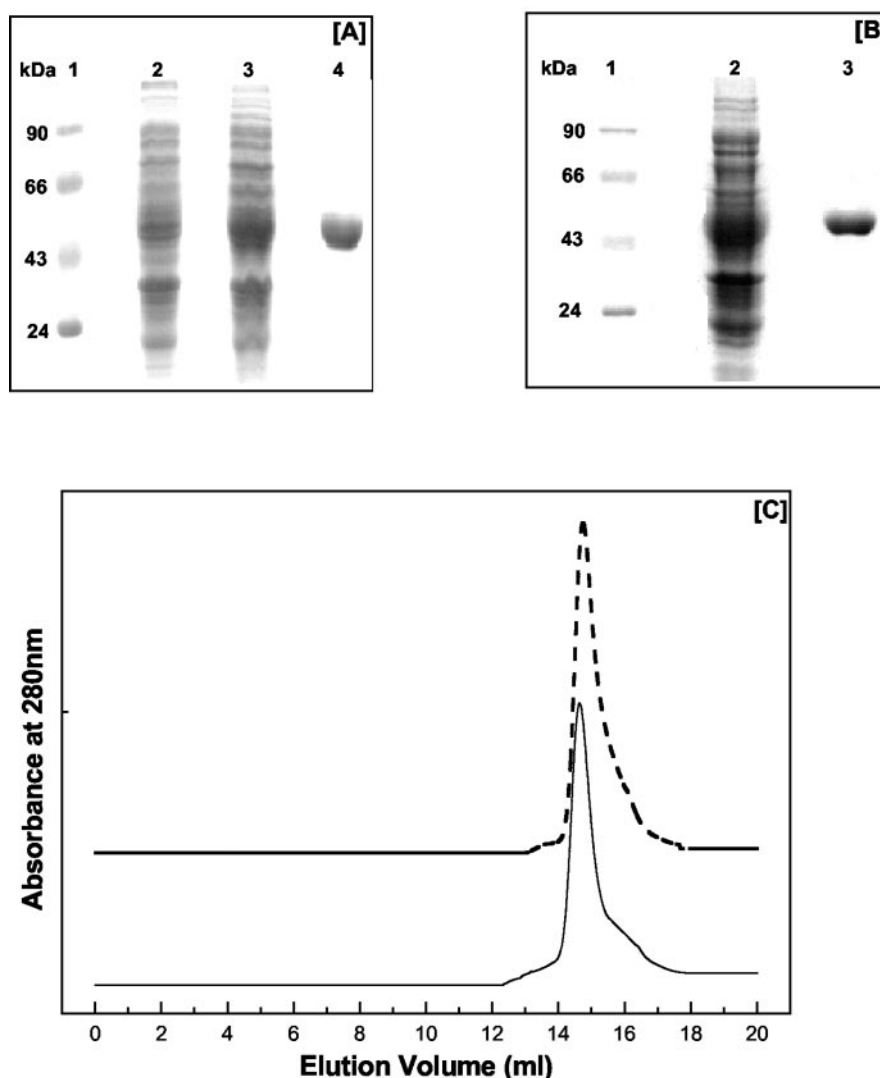


FIG. 1. SDS-PAGE analysis of *E. coli* lysate overexpressing SHM1 (panel A) and SHM2 (panel B) and the purified proteins. In panel A, lanes 1–4, represent molecular weight markers, uninduced culture, induced culture, and purified protein, respectively. In panel B, lanes 1–3, represent molecular weight markers, uninduced culture, and purified protein, respectively. Panel C represents size-exclusion chromatographic profiles for SHM1 (solid line) and SHM2 (dashed line) on the Superdex 200HR column at pH 7.6 and 25 °C. The experimental details are given under “Experimental Procedures.”

nant SHM1 and SHM2, respectively, which is within the limits of the values reported for SHMT from various sources (24).

Molecular Weight and Subunit Structure

The molecular masses of the purified recombinant SHM1 and SHM2 were determined under non-dissociating conditions as described by Andrews (25) using the data of gel filtration experiments. Gel filtration of SHM1 and SHM2 on a Superdex S-200 column, calibrated with the various molecular weight standards, showed a single peak although with a slight difference in retention volume of 14.55 and 14.7 ml, respectively, for the two enzymes (Fig. 1C). When the elution volumes of the marker proteins were plotted as a function of log of molecular masses, the molecular masses of 91.2 and 87.1 kDa were obtained for SHM1 and SHM2, respectively.

From the primary amino acid sequence, the molecular masses of 45.03 and 45.52 kDa were obtained for SHM1 and SHM2, respectively. The subunit masses of purified SHM1 and SHM2 were determined by SDS-PAGE. A single homogeneous protein band corresponding to molecular mass of about 45 kDa was observed for the two proteins (Fig. 1, A and B). The precise molecular weights of the two recombinant enzymes were obtained by ESI-MS experiments (data not shown). Molecular masses of 45.0 and 45.5 kDa were observed for SHM1 and SHM2, respectively, demonstrating that both the recombinant enzymes have very similar molecular masses.

The results of the studies on subunit masses along with the

size exclusion chromatography as reported above demonstrate that both SHM1 and SHM2 exist as dimers under physiological conditions. Furthermore, as both the proteins have similar molecular masses but significant differences are observed in their retention volumes (on size exclusion chromatography), it suggests that significant differences exist in the molecular dimensions of the two recombinant enzymes with SHM2 having a slightly more compact conformation (higher retention volume) than the SHM1 under physiological conditions.

Content of PLP

The SHMT is a PLP-dependent enzyme in which the PLP is covalently attached to the enzyme, bound as an aldimine to Lys-299 that is conserved in SHMT from various sources (12–14). Visible CD studies on SHMT have shown that the visible CD signal is different between the holo- and the apo- or unfolded enzyme. The holoenzyme has a unique peak at 425 nm because of the bound PLP, which disappears on unfolding of the enzyme or on removal of PLP from the enzyme, *i.e.* on stabilization of apoenzyme (16). The visible CD spectra of SHM1 and SHM2 are shown in Fig. 2A. For both the recombinant proteins a visible CD spectra centered at about 430 nm, showing the presence of the enzyme-bound PLP, was observed. However, at a similar enzyme concentration the visible CD signal for SHM2 was about 8 times greater than that observed for the SHM1 indicating that it probably has a higher content of PLP as compared with SHM1. To confirm this, the amount of PLP

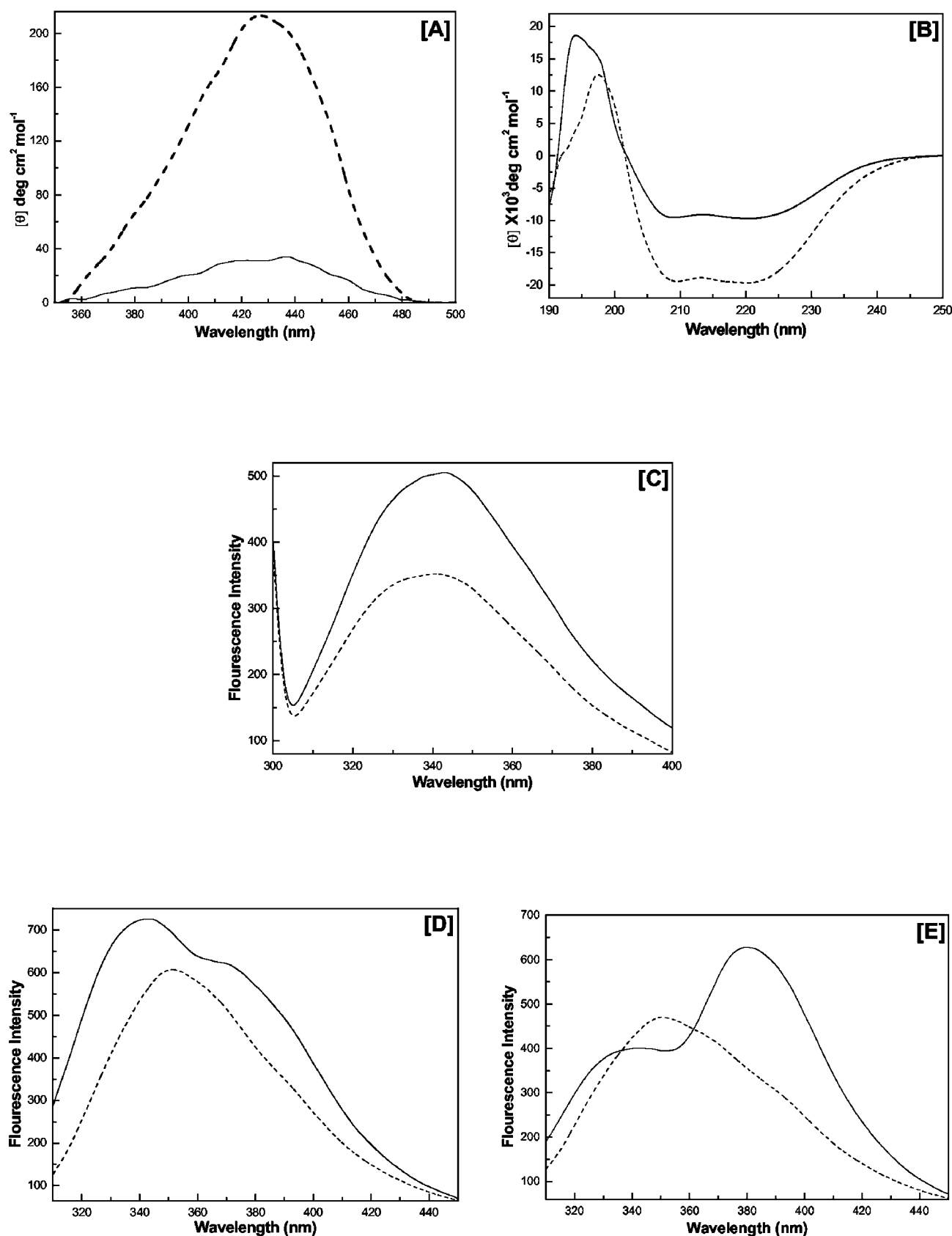


FIG. 2. CD and fluorescence properties of SHM1 and SHM2 at pH 7.6 and 25 °C. A, visible CD spectra of native recombinant proteins. B, far-UV CD spectra of native recombinant proteins. C, tryptophan fluorescence emission spectra of native recombinant proteins. In all the figures the solid lines represent data for SHM1 and the dashed line that for SHM2. Fluorescence emission spectra of native, pH 7.6, and unfolded (in presence of 8 M urea) PyP-SHM1 (panel D) and PyP-SHM2 (panel E). In both figures, the solid lines represent data for native protein and dashed lines for unfolded protein.

SHM1	-----MSAPLAEVDPDIAELLAKELG	21
SHM2	-----MNTLNDLSLAFDPDIAALIDGELR	24
E.coli	-----MLKREMNIAADYDAELWQAMEQEKV	24
B.subtilis	-----MKHLPAQDEQVFNIAIKNERE	20
Human cytoplasmic	-----MTMPVNGAHKDADLWSSSHDK-----MLAQPLKDS DVEVYNI IKKESN	42
Human mitochondrial	MLYFSLFWAARPLQRCGQLVRMAIRAQHSNAAQTQTGEANRGWTGQESLSDSDPEMWELLQREKD	65
SHM1	RQRDTLEMIASENFVPRVLAQAQGSVLTNKYAEGLPGRRYYGGCEHVDVVENLARDRAKALFGAE	86
SHM2	RQESGLEMIASENYAPLAVMQAQSGLTNKYAEGYPGRRYYGGCEFDVGEQLAIDRVKALFGAE	89
E.coli	RQEEHIELIASENYTSRPMVQAQGSGLTNKYAEGYPGKRRYYGGCEYVDIVEQLAIDRAKELFGAD	89
B.subtilis	RQQTKEILIASENFVSEAVMEAQGSGLTNKYAEGYPGKRRYYGGCEHVDVVEDIARDRAKEIFGAE	85
Human cytoplasmic	RQRVGLELIASENFASRAVLEALGSLNNKYSEGYPGQRYYGGTEFIDELETLCKRALQAYKLD	107
Human mitochondrial	RQCRGLELIASENFCSSRAALEALGSLNNKYSEGYPGKRRYYGGAEEVVDIEELLCQRRALEAFDLD	130
SHM1	----FANVQPHSGAQANAAVLHALMSPGERLLGLDLANGGHLTHG-----MRLNFSGKLYENGIFY	142
SHM2	----YANVQPHSGATANAATMHALLNPGDTILGLSLAHGGHLTHG-----MRINFSGKLYHATAY	145
E.coli	----YANVQPHSGSQANFAVYTALLEPGDTVLGMNLAHGGHLTHG-----SPVNFSGKLYNIVPY	145
B.subtilis	----HVNVPQPHSGAQANMAVYFTILEGQDVTVLGMNLSHGGHLTHG-----SPVNFSGVQYNFVEY	141
Human cytoplasmic	PQCWGVNVQPYSGSPANFAVYTALVEPHGRIMGLDLPDGGHLTHGFMTDKKKISATSIFFESMPY	172
Human mitochondrial	PAQWGVNVQPYSGSPANLAVYTALLQPHDRIMGLDLPDGGHLTHGYMSDVKKISATSIFFESMPY	195
SHM1	GVDPATHLIDMDAVRATALEFRPKVIIAGWSAYPRVLDFAAFRSIADEVGAKLLVMAHFAVLVA	207
SHM2	EVSKEGYLVMDDAVAEAAARTHRPKMIIAGWSAYPRQLDFARFRAIADEVDAVLVMAHFAVLVA	210
E.coli	GID-ATGHIDYADLEKQAKEHKPKMIIIGGFSAYSGVVDWAKMREIADSIAGLVFVMAHFAVLVA	209
B.subtilis	GVDKETQYIDYDDVREKALAHKPKLIVAGASAYPTIDFKKFREIADEVGAYFMVMAHIAVLVA	206
Human cytoplasmic	KVNPDTGYINYDQLEENARLFHFKLIAGTSCYSRNLEYARLRKIADENGAYLMADMAHISGLVA	237
Human mitochondrial	KLNPKTGLIDYNQLALTARLFRPLIIAGTSAAYARLIDYARMREVCEVKAHLADMAHISGLVA	260
SHM1	AGLHPSVPVHADVVSTTHKTLGGGRSGLIVG-----KQOYAKAINSAVFPQQG	257
SHM2	AGVHPSVPVHAHVVTSTTHKTLGGPRGGIILCN-----DPAIAKKINSAVFPQQG	261
E.coli	AGVYPNPVPHAHVVTSTTHKTLAGPRGGLILAKG-----GSEELYKKLNSAVFPQQG	262
B.subtilis	AGLHPNPVPYADFVTSTTHKTLRGRGGMILCR-----EEFGKKIDKSIFFPIQG	256
Human cytoplasmic	AGVVPSPFEHCHVVTSTTHKTLRGCRAGMIFYRKGVKSVDPKTGKEILYNLESINSVFPGLQG	302
Human mitochondrial	AKVIPSPFKHADIVTSTTHKTLRGLARSGLIFYRKGVKAVDPKTGREIPYTFEDRINFVFPFLQG	325
SHM1	GPLMHVIAAGKAVALKIAATPEFADRQRRTLSGARIADRLMAPDVAAGVSVVSGGTDVHLVLVD	332
SHM2	GPLEHVIAAKATAFKMAAQPEFAQRQRCCLDGARILAGRLTQPDVAERGIAVLTGGTDVHLVLVD	326
E.coli	GPLMHVIAAGKAVALKAMEPEFKTYQQQVAKNAKAMVEVFL-----ERGYKVVSGGTDNHLFLVD	322
B.subtilis	GPLMHVIAAKAVSFGEVLQDDFKTYAQNVISNAKRLAEALT-----KEGIQLVSGGTDNHLILVD	316
Human cytoplasmic	GPHNHAIAGVAVALKQAMTLEFKVYQHQQVANCRALEALT-----ELGYKIVTGGSDNHLILVD	362
Human mitochondrial	GPHNHAIAAVAVALKQACTPMFREYSIQVLKNARAMADALL-----ERGYSLVSGGTDNHLVLVD	385
SHM1	LRDSPLDGQAAEDLLHEVGITVNRNAVNDPRPPMVTSGLRIGTPALATRGFGDTEFTEVADIIA	387
SHM2	LRDAELDGQAAEDRLAAVDITVNRNAVFPDPRPPMITSGLRIGTPALAARGFSHNDFRAVDLIA	391
E.coli	LVDKNLTGKEADAALGRANITVNKNSVPNDPKSPFVTSGIRVGTPAITRRGFKEAEAKELAGMMC	387
B.subtilis	LRSGLTGKVAEHVLEIGITSNKNAIPYDEPKPFVTSGIRLGTAAVTSRGFDGDALEEVGAI	381
Human cytoplasmic	LRSKGTGGRAEKVLEACSIACNKNTCPGD-RSALRPSGLRLGTALTSTRGLEKDFQKVAFHFIH	426
Human mitochondrial	LRPKGLDGARAERVLELVISITANKNTCPGD-RSAITPGGLRLGAPALTSTRQFREDDFRRVDFID	449
SHM1	TALATGSS-----VDVSALKDRATRLARAFPLYDGLLEWVSLVGR	426
SHM2	AALTATND-----DQLGPLRAQVQRLAARYPLYPELHRT	425
E.coli	DVLDSINDE-----AVIERIKGVLDICARYPVYA	417
B.subtilis	LALKNHED-----GKLEEARQVAALTDKFPLYKELDY	415
Human cytoplasmic	RGIELTLQIQSDTGVRATLKEFKERLAGD-KYQAAVQALREEVESFASLFPPLPDF	483
Human mitochondrial	EGVNIGLEVSKT---AKLQDFKSFLLKDSSETSQRLANLRQVEQFARAFPMGPFDEH	504

FIG. 3. Alignment of the amino acid sequence of SHMT from various sources. The alignment was done with the software CLUSTALW. The arrow denotes the site of the octapeptide having five threonine residues, which is conserved in all SHMT except SHM1 and SHM2. The light shaded letters indicate the amino acids involved in binding of enzyme to the PLP.

bound to the enzyme was determined for both recombinant enzymes by the method of Urevitch and Kallen (25) after extensive dialysis of the purified recombinant enzymes against 25 mM potassium phosphate buffer, pH 7.6, 50 mM NaCl, and 1 mM EDTA. The SHM1 and SHM2 were found to contain 1 ± 0.2 and 2.3 ± 0.5 mol of PLP/mol of enzyme, respectively.

The SHMT from mammalian sources are homotetramers and contain 4 mol of PLP/mol of enzyme (12, 13), whereas the SHMT from *E. coli* as well as from other bacterial sources are dimeric and contain 2 mol of PLP/mol of enzyme (14). All the SHMTs reported to date including SHM2 (reported in this paper) contain 2 mol of PLP/mol of enzyme dimer, however, SHM1 was found to contain only 1 mol of PLP/mol of enzyme dimer. This is the first report on such a unique stoichiometry of PLP and enzyme for SHMT.

Comparative Structural and Functional Properties of the Recombinant SHM1 and SHM2

Secondary Structure—Far-UV CD studies were carried out on both SHM1 and SHM2 to analyze the differences in the secondary structure that exist between the two enzymes. For both SHM1 and SHM2, the far-UV CD spectra characteristic of a protein having both α -helix and β -sheet secondary structure was observed (Fig. 2B). However, for similar molar concentrations of enzyme, a significantly higher ellipticity was observed for SHM2 over the whole far-UV region (Fig. 2B). This observation suggests that SHM2 have a significantly higher secondary structure as compared with SHM1. Despite having similar subunit molecular mass as SHM1, the SHM2 was found to have a more compact conformation. One possible reason for this may

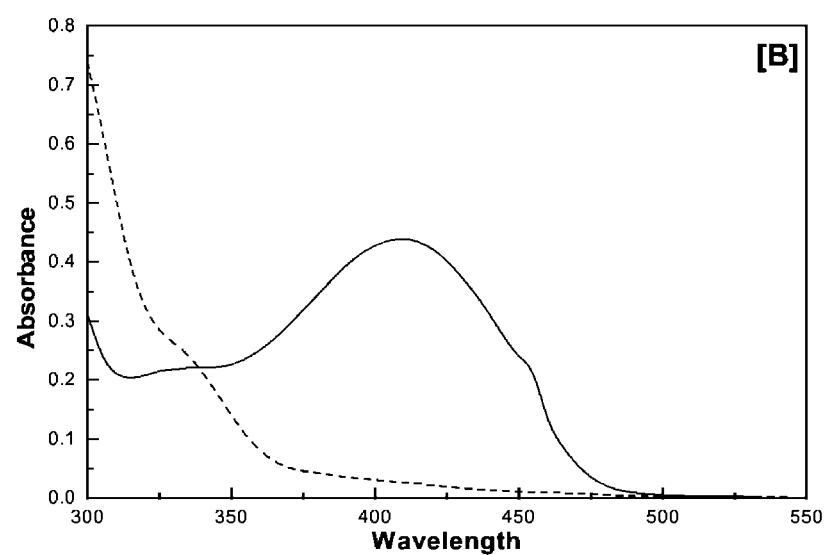
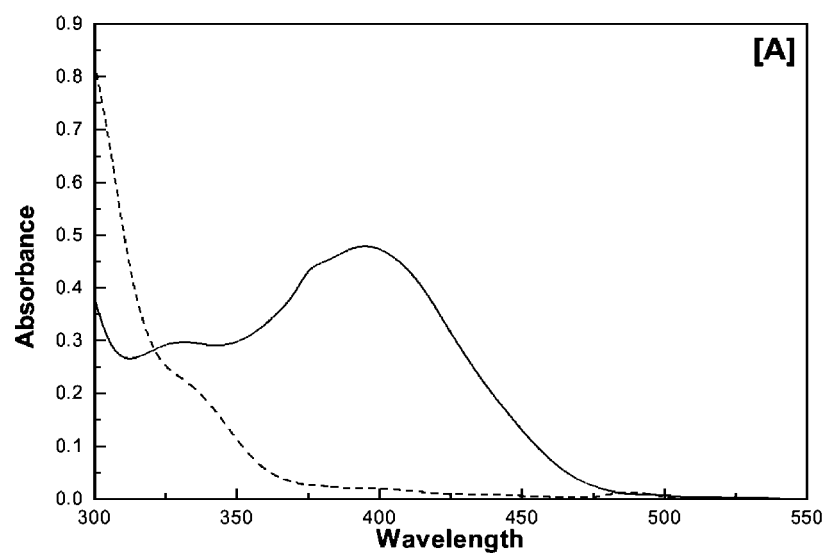


FIG. 4. Comparative analysis of functional properties of SHM1 and SHM2 at pH 7 and 25 °C. Effect of L-cysteine on the absorption spectra of SHM1 (panel A) and SHM2 (panel B). In both A and B the solid curves represent absorption spectrum of enzyme (5 μ M) in 0.01 M potassium phosphate, pH 7.6, and the dashed curve represents absorption spectra of enzyme after addition of 100 mM L-cysteine and incubation for 20 min. C, pH-induced changes in enzyme activity of SHM1 (triangles) and SHM2 (circles). The experimental details are given under "Experimental Procedures."

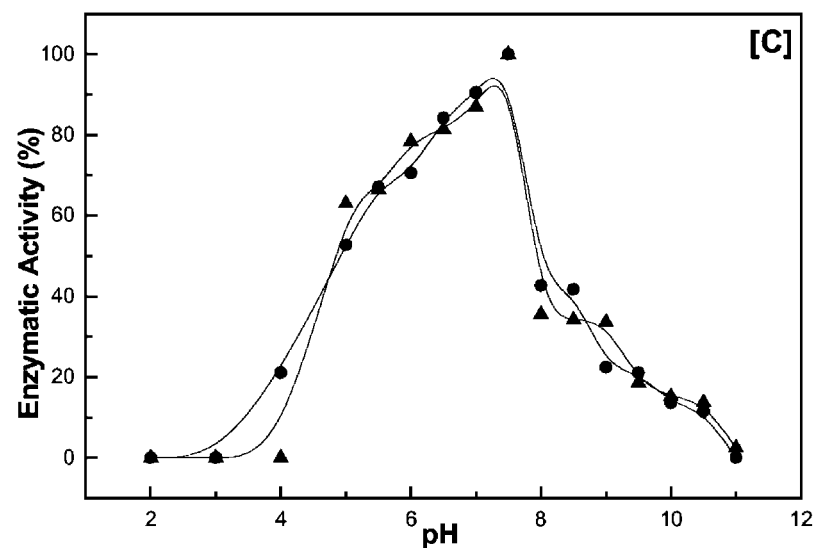
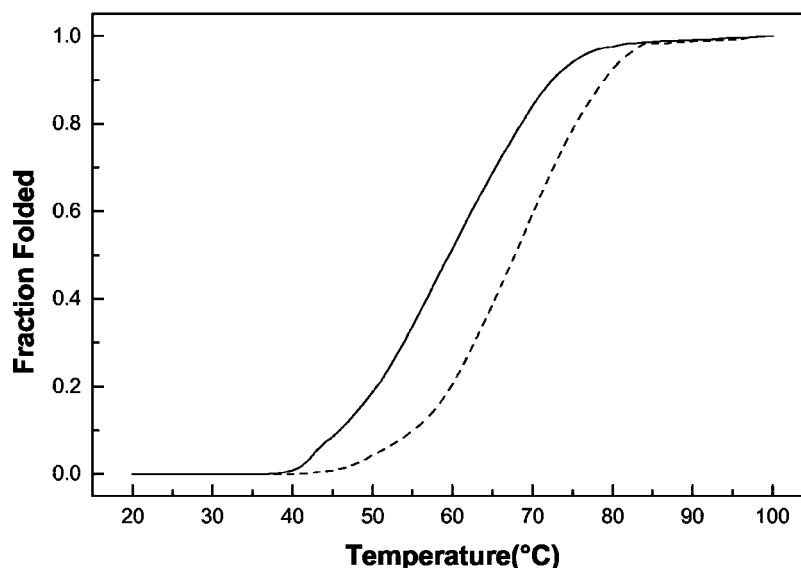


FIG. 5. **Thermal denaturation of native recombinant enzymes measured by loss of CD ellipticity at 222 nm.** A linear extrapolation of baselines in pre- and post-transitional regions was used to determine the fraction-unfolded protein within the transition region by assuming a two-state mechanism of unfolding. The solid and dashed lines represent data for SHM1 and SHM2, respectively. The thermal transition was found to be irreversible and the precipitation of the recombinant enzymes was observed at about 90 °C irrespective of the buffer used.



be the presence of a significantly higher secondary structure in SHM2, which would result in stabilization of a compact conformation.

Tryptophan Fluorescence—According to the primary amino acid sequence, SHM1 has two tryptophan molecules at positions 172 and 421, whereas SHM2 has a single tryptophan at position 175. The fluorescence spectra of SHM1 and SHM2 are shown in Fig. 2C. For both the enzymes the emission wavelength maxima for the tryptophan fluorescence was observed at about 339 nm, however, there were significant differences in fluorescence intensities of the two enzymes because of the difference in number of tryptophan moieties present in them. The buried tryptophan residues in folded protein show fluorescence emission maxima at 330–335 nm, whereas on unfolding of protein the tryptophan fluorescence emission maxima shifts to about 350 nm (27). Hence, both in SHM1 and SHM2 the tryptophan molecule(s) is not completely buried but partially exposed to the solvent.

Fluorescence Resonance Energy Transfer—For eSHMT it has been demonstrated that reduction of the PLP aldimine bond results in absorbance maxima at 355 nm that overlaps the emission spectrum of tryptophan. Hence, the PyP can be used as an energy acceptor of tryptophan fluorescence. For native eSHMT FRET is observed that abolishes on unfolding of enzyme (20). Fig. 2, D and E, summarizes the results of FRET experiments on SHM1 and SHM2. For both the SHM1 and SHM2 in the native conformation two emission maxima, one around 339 nm (tryptophan fluorescence) and the other at 385 nm (PyP emission resulting from FRET) were observed. However, on unfolding of enzymes by incubation in 8 M urea only single emission maximum at 352 nm was observed. These observations demonstrate that for SHM1 and SHM2 in the native conformation there is FRET between tryptophan residues and the bound PLP suggesting that the tryptophan residue(s) is located less than 5 Å from PyP in the native conformation of these two enzymes and on denaturation of the enzymes these two moieties move apart resulting in the loss of FRET.

Functional Properties—All the forms of SHMT for which a primary sequence is known contain the eight-residue conserved sequence, VTTTTHK(Pyr)/T, near the active-site lysyl residue (Lys-229 as in eSHMT) that forms the internal aldimine with pyridoxal phosphate. The active site octa-peptide from SHMT is unusual in the sense that it has five threonine residues conserved in all the reported primary sequence of SHMTs (Fig.

3). Mutation studies have demonstrated that Thr-226 plays an important role in converting the *gem*-diamine complex to external aldimine complex. A T226A mutant of eSHMT has been shown to distinguish between substrates and substrate analogs in formation of the *gem*-diamine complex (28). The primary sequence of SHM1 and SHM2 show significant changes in the conserved threonine sequence (Fig. 3). In SHM1, the Thr-225 (corresponding to Thr-227 of eSHMT) and Thr-222 (corresponding to Thr-224 of eSHMT) are replaced with valine and serine, respectively. In SHM2 the Thr-226 (corresponding to Thr-225 of eSHMT) is replaced by serine (Fig. 3). These alterations may lead to significant changes in substrate binding and complex formation in these enzymes.

It has been reported that D-alanine reacts with SHMT to undergo a slow half-transamination reaction resulting in the formation of apoenzyme, pyridoxamine-P, and pyruvate (29). Experimentally this reaction is detected by a decrease of the absorption at 410 nm (present in native SHMT) and appearance of an absorption peak at 327 nm on incubation of SHMT with D-alanine (29). Incubation of approximately 100 mM D-alanine did not result in any change in absorption intensity at 410 nm for the native SHM1 or SHM2 (data not shown), which demonstrates that D-alanine does not react with either SHM1 or SHM2.

L-Cysteine has been shown to be an agent, which can be used to resolve the SHMT at neutral pH probably by combining with the enzyme-bound PLP and forming a more stable thiazolidine complex (30). Experimentally this reaction is detected by decrease of absorption at 410 nm (present in the native SHMT) and appearance of an absorption peak at 330 nm on incubation of SHMT with L-cysteine. Fig. 4, A and B, shows the absorption spectra of SHM1 and SHM2 and on incubation with L-cysteine. Incubation of SHM1 and SHM2 with 100 mM L-cysteine resulted in absolute loss of absorption intensity at 410 nm for both the recombinant enzymes and appearance of an absorption peak at 330 nm demonstrating that the enzyme-bound PLP in SHM1 or SHM2 has been removed by L-cysteine.

The pH dependence of the enzymatic activity of SHM1 and SHM2 was studied and is summarized in Fig. 4C. For both enzymes, bell-shaped curves centered at about pH 7.8 were observed. Furthermore, a complete loss of activity was observed at pH below 4.0 and above 10.0. These observations demonstrate that both SHM1 and SHM2 have similar pH optima for the enzymatic activity.

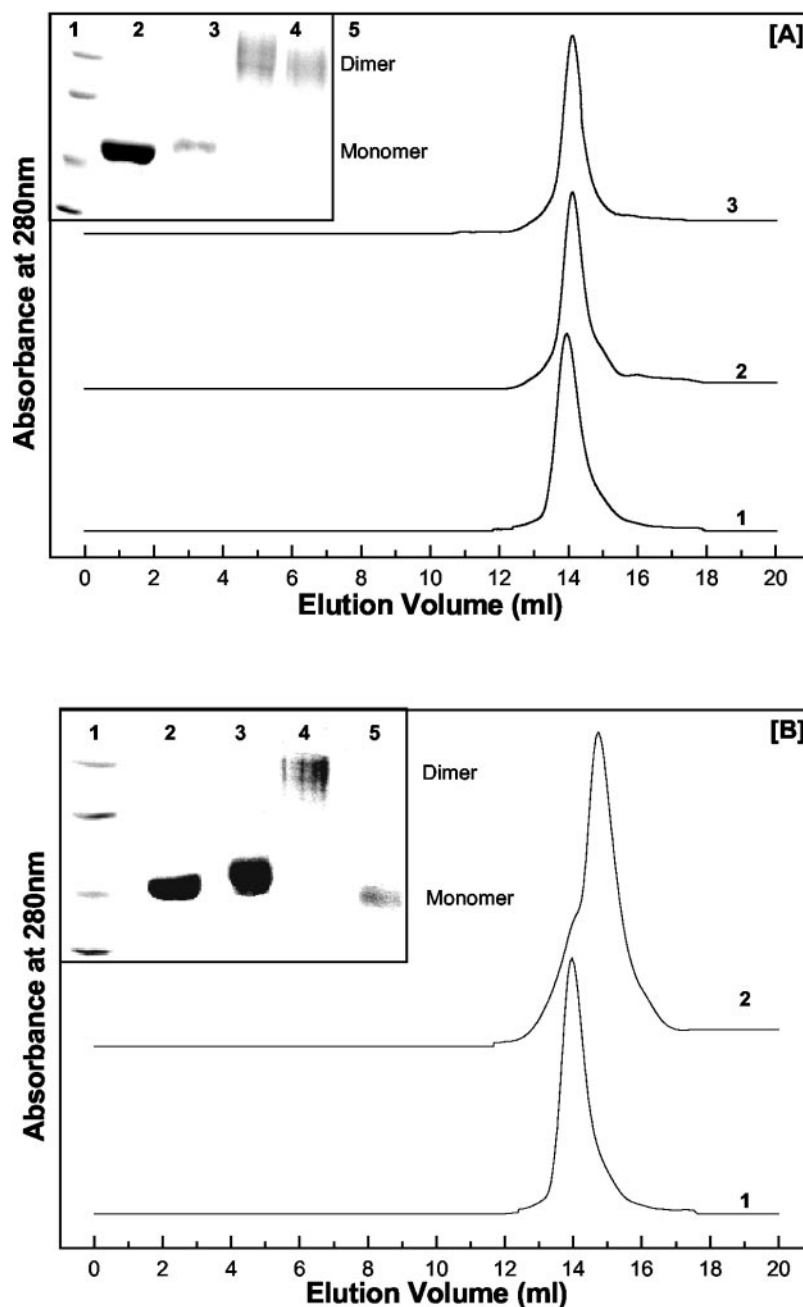


FIG. 6. pH-induced alterations in molecular dimension and subunit configuration of SHM1 and SHM2. *A*, size-exclusion chromatographic profiles for SHM1 on Superdex 200HR column at increasing pH. The curves 1–3 represent profiles for pH 7.6-, 9-, and 10.5-treated SHM1 protein samples, respectively. *B*, size-exclusion chromatographic profiles for SHM2 on the Superdex 200HR column at increasing pH. Curves 1 and 2 represent profiles for pH 7.5- and 9-treated SHM2 protein samples. For these studies citrate/glycine/Hepes buffer (10 mM each) was used and the desired pH was maintained with 1 N NaOH or HCl. The columns were run at the pH at which the protein samples were incubated. In both figures the insets show SDS-PAGE profiles of glutaraldehyde cross-linked pH 3–10.5-treated protein samples. Lanes 1 and 2 represent molecular weight markers, and uncross-linked native protein, respectively and lanes 3–5 represent cross-linked samples of pH 3-, 7.5-, and 10-treated protein, respectively.

Comparative Denaturation Studies on SHM1 and SHM2

Thermal Denaturation—The thermal unfolding of SHM1 and SHM2 were characterized by monitoring the loss of secondary structure of enzymes with temperature. Fig. 5 summarizes the changes in CD ellipticity at 222 nm for SHM1 and SHM2 at increasing temperatures. For both enzymes, a single irreversible sigmoidal transition was observed suggesting a cooperative thermal unfolding of native enzyme dimer to unfolded monomer. Furthermore, for both enzymes the transition was observed in the temperature region 40–80 °C, however, it was centered at about 60 and 69.4 °C for SHM1 and SHM2, respectively. As a difference of about 9 °C in the T_m was observed for the two enzymes it demonstrates that SHM2 has higher thermal stability than SHM1, which is probably because of the presence of a more compact native conformation having higher secondary structure than SHM1.

pH-induced Denaturation—Far-UV and visible CD studies on SHM1 and SHM2 at increasing pH were performed to study

the pH-induced alterations in the secondary structure and the PLP-binding site of the two enzymes. In the pH range between 4 and 5, aggregation was observed for both enzymes (data not shown). However, at about pH 3.0, monomers of both enzymes were found to be stabilized (glutaraldehyde cross-linking experiments summarized in Fig. 6, *A* and *B*, inset). In contrast, in the alkaline pH range significant differences in the structural properties of the two enzymes were observed. Because of this reason structural changes in the recombinant enzymes in the alkaline pH range are being discussed in detail.

Fig. 7A summarizes the effect of increasing pH, between pH 6 and 11, on the CD ellipticity at 222 nm for SHM1 and SHM2. For SHM2, a sigmoidal transition was observed between pH 8 and 10 with about 50% loss of the CD ellipticity at 222 nm associated with this transition. In contrast, for SHM1 no significant alteration in CD ellipticity at 222 nm was observed between pH 6 and 11. These results demonstrate that secondary structure of native SHM1 is not significantly affected by

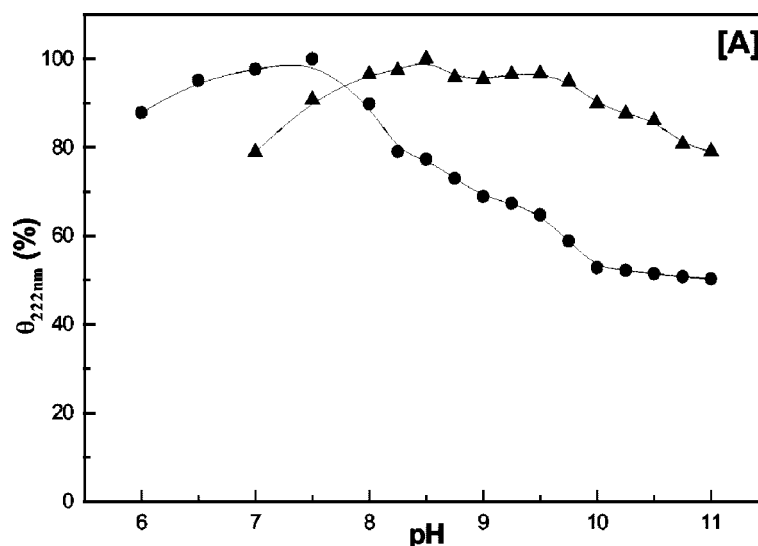
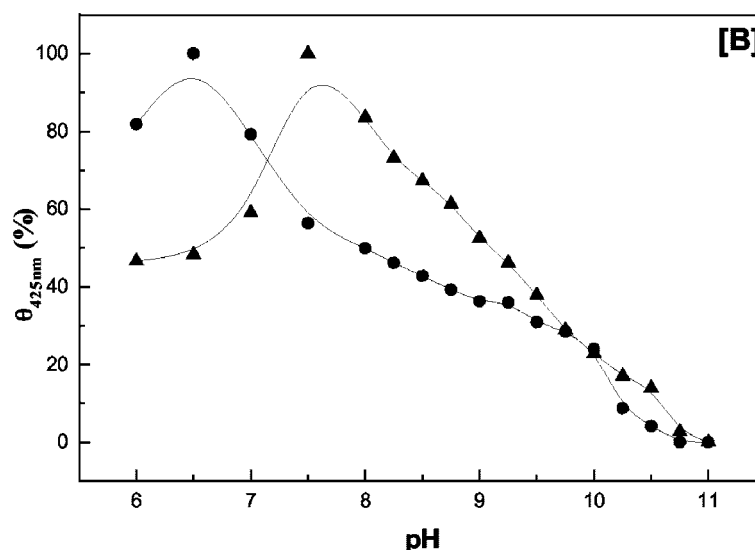


FIG. 7. A, pH-induced changes in secondary structure of SHM1 (triangles) and SHM2 (circles) as monitored by following the changes in ellipticity at 222 nm obtained from far-UV CD curves at increasing pH. B, pH-induced changes to enzyme-bound PLP of SHM1 (triangles) and SHM2 (circles) as monitored by following the changes in ellipticity at 425 nm obtained from visible CD spectra at increasing pH.



enhancing the pH to 11.0, however, for SHM2 a significant denaturation occurs under similar conditions.

Fig. 7B summarizes the changes in visible CD signal of SHM1 and SHM2 between pH 6 and 11. For both enzymes, a sigmoidal transition for loss of CD signal in the visible region was observed in the alkaline pH region. However, for SHM2 the transition was observed between pH 6.5 and 11 centered at pH 8.0, whereas for SHM1 it was between pH 8 and 11 centered at about pH 9.25. These results demonstrate that compared with SHM2, the SHM1 shows higher stability against alkaline denaturation. Furthermore, for both SHM1 and SHM2 a complete loss of visible CD signal was observed at about pH 10 and above suggesting that at high pH the enzyme-bound PLP molecule gets dissociated from both recombinant enzymes resulting in stabilization of apoenzymes.

For studying the effect of alkaline pH on the molecular dimensions of the native SHM1 and SHM2, size exclusion chromatographic studies were carried out. Fig. 6, A and B, summarizes the elution profile of SHM1 and SHM2 on the

S-200 Superdex column between pH 7.5 and 10.0. For native SHM1 at pH 7.5, a single peak with a retention volume of 14.06 ml corresponding to the dimeric species of enzyme was observed. On increase in pH from 7.5 to 10.5, no significant changes in the retention volumes of the native SHM1 were observed (Fig. 6A). This suggests that no significant alteration in the molecular dimension or subunit configuration of SHM1 occurs on enhancement of pH in alkaline region. This was confirmed by the glutaraldehyde cross-linking studies where a single protein band corresponding to that of the dimer of the enzyme was observed between pH 7.5 and 10.5 (Fig. 6A, inset). In contrast for SHM2, on increase in pH from 7.5 to 9 an enhancement in the retention volume from 14.13 to 15.2 ml was observed (Fig. 6B). The enhancement in the retention volume for pH 9-treated SHM2 compared with the native enzyme is indicative of significantly reduced hydrodynamic radii for the stabilized enzyme intermediate under these conditions. On comparing the elution volume of pH 9.0-treated SHM2 with the molecular mass obtained for marker proteins in the size

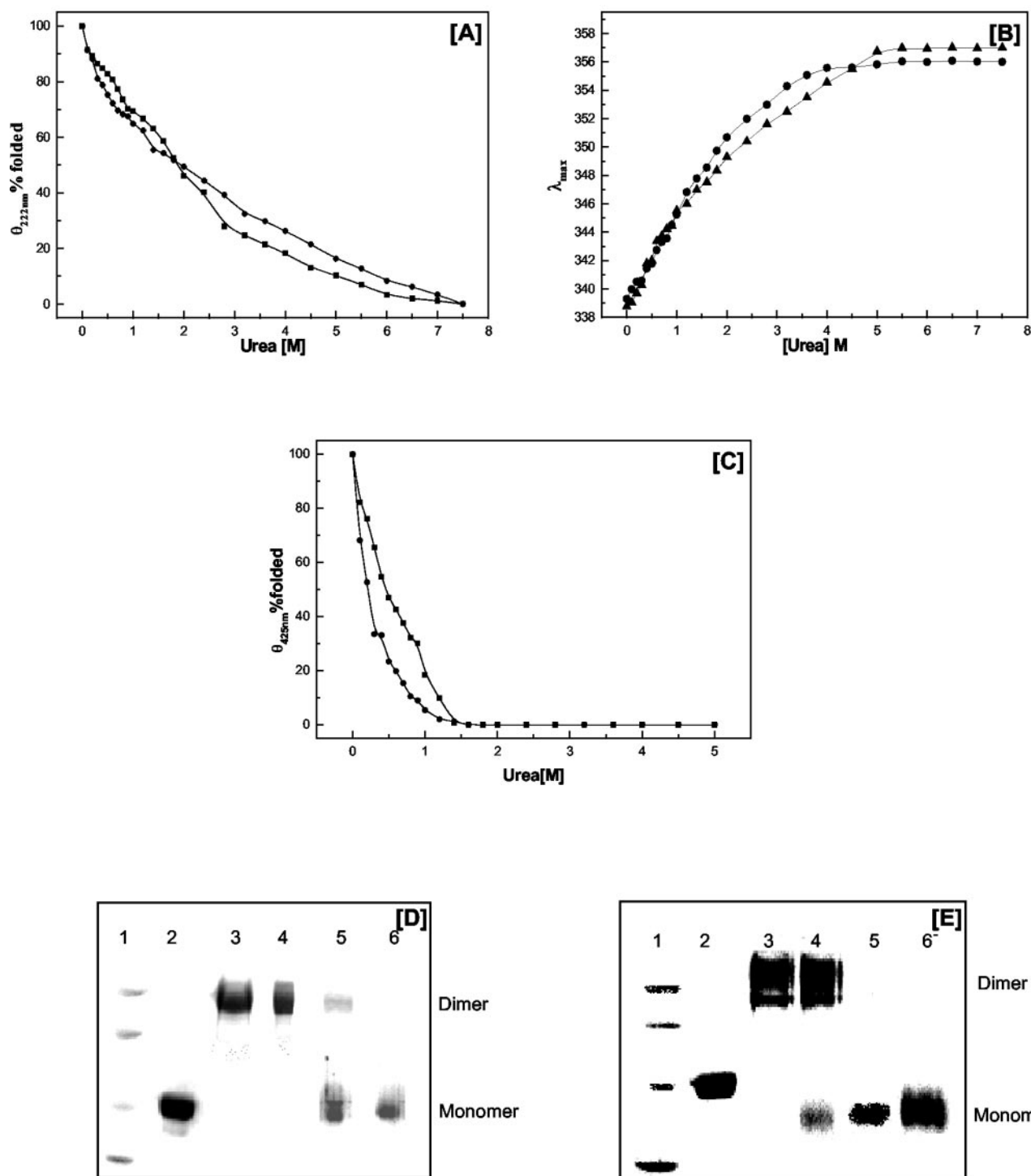


FIG. 8. A, urea-induced changes in secondary structure of SHM1 (triangles) and SHM2 (circles) as monitored by following the changes in ellipticity at 222 nm obtained from far-UV CD curves at increasing concentrations of urea. B, changes in the wavelength of maximum fluorescence emission of tryptophans of SHM1 (triangles) and SHM2 (circles) versus urea concentration. C, urea-induced changes in enzyme-bound PLP of SHM1 (triangles) and SHM2 (circles) as monitored by following the changes in ellipticity at 425 nm obtained from visible CD spectra at increasing the concentrations of urea. Panels D and E show SDS-PAGE profiles of glutaraldehyde cross-linked urea-treated SHM1 and SHM2, respectively. In both the figures, lanes 1 and 2 represent molecular weight markers and uncross-linked native protein, respectively, and lanes 3–6 represent cross-linked samples of 0, 0.8, 1.6, and 2 M urea-treated protein samples, respectively.

exclusion chromatography (with citrate/glycine/Hepes buffer), a molecular mass of about 45 kDa was obtained. As the SHM2 monomer has a molecular mass of about 45 kDa (Fig. 1), these observations indicate that alkaline treatment of SHM2 probably leads to dissociation of native dimer of enzyme resulting in stabilization of the enzyme monomer. This possibility was confirmed by the glutaraldehyde cross-linking studies where a

single protein band corresponding to monomer of enzyme was observed on SDS-PAGE for pH 9-treated SHM2 (Fig. 6B, inset).

Urea-induced Denaturation—The urea-induced denaturation of SHM1 and SHM2 were studied by monitoring the changes in the secondary structure, the tertiary structure, and the enzyme-bound PLP of the recombinant proteins at increasing urea concentrations. Fig. 8A summarizes the changes in the

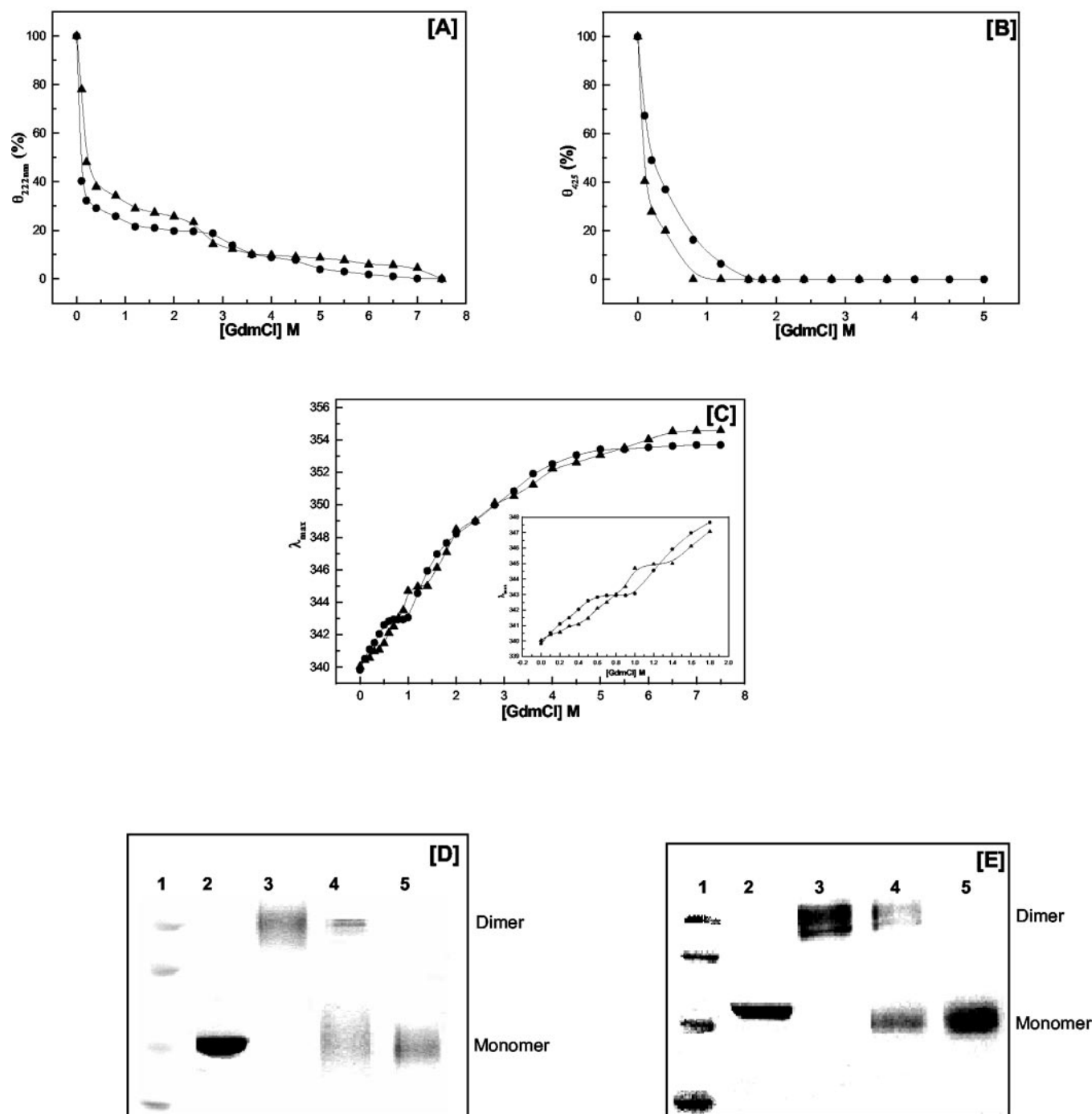


FIG. 9. A, GdmCl-induced changes in secondary structure of SHM1 (triangles) and SHM2 (circles) as monitored by following the changes in ellipticity at 222 nm obtained from far-UV CD curves at increasing concentrations of GdmCl. B, GdmCl-induced changes of enzyme-bound PLP of SHM1 (triangles) and SHM2 (circles) as monitored by following the changes in ellipticity at 425 nm obtained from visible CD spectra at increasing concentrations of GdmCl. C, changes in the wavelength of maximum fluorescence emission of tryptophans of SHM1 (triangles) and SHM2 (circles) versus GdmCl concentration. The inset shows the changes between 0 and 2 M GdmCl. Panels D and E show SDS-PAGE profiles of glutaraldehyde cross-linked urea-treated SHM1 and SHM2, respectively. In both figures, lanes 1 and 2 represent molecular weight markers and uncross-linked native protein, respectively, and lanes 3–5 represent cross-linked samples of 0, 0.2, and 2 M GdmCl-treated protein samples, respectively.

far-UV CD signal of SHM1 and SHM2 on treatment with increasing concentrations of urea. For both enzymes, an exponential decrease in CD ellipticity at 222 nm between 0 and 6 M urea and complete loss of CD signal above 6.5 M urea were observed. These observations suggest that both SHM1 and SHM2 undergo a continuous loss of secondary structure on treatment with increasing concentration of urea.

The urea-induced alterations in tertiary structure of recombinant proteins SHM1 and SHM2 was studied by monitoring the changes in the tryptophan fluorescence emission wave-

length maxima at increasing concentrations of urea and are summarized in Fig. 8B. An exponential increase in tryptophan fluorescence emission wavelength maxima from 339 to 356 nm for both the SHM1 and SHM2 were observed with increasing urea concentrations between 0 and 5 M urea. These observations suggest that treatment of enzyme with increasing concentrations of urea lead to movement of partially buried tryptophan molecules present in the native enzyme toward the solvent (27). Such a situation can arise only when the enzyme molecule undergoes unfolding on treatment with urea. The

far-UV CD and tryptophan fluorescence results presented above collectively demonstrate that during the urea-induced denaturation a simultaneous unfolding of both the secondary and tertiary structures occurs in both SHM1 and SHM2.

The urea-induced changes in the enzyme-bound PLP of SHM1 and SHM2 was studied by monitoring the changes in the visible CD signal of the enzymes at increasing urea concentration. A sharp decrease in CD signal at 425 nm was observed between 0–1 and 0–1.2 M urea for SHM1 and SHM2, respectively. Above 1.25 M urea concentration, a complete loss of visible CD signal was observed for both recombinant enzymes suggesting that for both SHM1 and SHM2 the enzyme-bound PLP gets dissociated from the enzyme on treatment with about 1.25 M urea. However, at about 1.25 M urea only about 40% loss of CD ellipticity at 222 nm and partial exposure of tryptophan residues of enzyme to solvent was observed for the two enzymes. This indicates a possibility of stabilization of a partially unfolded apo-intermediate of SHM1 and SHM2 on treatment with low concentrations of urea.

The effect of urea on the subunit configuration of SHM1 and SHM2 was studied by carrying out glutaraldehyde cross-linking studies. Fig. 8, C and D, summarizes the results of the glutaraldehyde cross-linking results of the native and 1.6 M urea-treated SHM1 and SHM2. For 1.6 M urea-treated SHM2, a single protein band corresponding to monomer of enzyme was observed, whereas for SHM1 two protein bands corresponding to monomer and dimer, respectively, were observed. These observations in conjunction with the results of CD and tryptophan fluorescence studies demonstrate that treatment of SHM1 and SHM2 with low urea concentrations leads to dissociation of native dimer of these enzymes resulting in stabilization of an apomonomer.

Guanidinium Chloride-induced Denaturation

The GdmCl-induced denaturation of SHM1 and SHM2 was studied by monitoring the alterations in far-UV and visible CD and tryptophan fluorescence profiles of the two enzymes at increasing GdmCl concentrations. Fig. 9, A and B, summarizes the far-UV and visible CD changes in SHM1 and SHM2 between 0 and 5 M GdmCl. For both enzymes, a sharp exponential decrease in CD ellipticity at 425 nm with increasing GdmCl concentrations were observed between 0 and 1.25 M GdmCl. Above 1.5 M GdmCl a complete loss of visible CD signal for SHM1 and SHM2 were observed suggesting dissociation of the enzyme-bound PLP under these conditions. However, for CD ellipticity at 222 nm an initial sharp loss of about 60% of signal was observed between 0 and 0.5 M GdmCl followed by a gradual loss of ellipticity between 0.75 and 4 M GdmCl. As the GdmCl concentration at which the dissociation of enzyme-bound PLP was found to occur only about 60% loss of secondary structure of enzyme was observed, these observations indicate a possibility of stabilization of a partially unfolded intermediate during GdmCl denaturation of both enzymes (31).

The stabilization of a partially unfolded intermediate of SHM1 and SHM2 during GdmCl-induced unfolding of enzymes was further supported by the tryptophan fluorescence studies. Fig. 9C shows the changes in tryptophan fluorescence emission wavelength maxima on treatment of SHM1 and SHM2 in the presence of increasing concentrations of GdmCl. For both SHM1 and SHM2, two distinct transitions were observed between GdmCl concentrations of 0 and 6 M. For SHM1 the two transitions were in the GdmCl concentration ranges 0–1.5 and 1.5–6 M, whereas for SHM2 they were in the GdmCl concentration ranges 0–1 and 1.1–7 M. At GdmCl concentration about 5 M and above the tryptophan fluorescence emission wavelength maxima of about 354 nm was observed suggesting com-

plete unfolding of enzymes under these conditions (27).

The subunit configuration of the GdmCl-stabilized intermediate of SHM1 and SHM2 was characterized by glutaraldehyde cross-linking experiments and are summarized in Fig. 9, D and E. For 0.2 M GdmCl-treated SHM1 and SHM2, two protein bands corresponding to dimer and monomer, respectively, of the recombinant enzymes were observed. However, for SHM1 the population corresponding to the monomer of the enzyme was significantly higher compared with that for the dimer (Fig. 9D). In contrast for SHM2 an almost equal population of the monomer and dimer was observed (Fig. 9E). The above reported observations collectively demonstrate that treatment of SHM1 and SHM2 with low concentrations of GdmCl lead to dissociation of the native dimer of enzymes along with dissociation of enzyme bound PLP, resulting in stabilization of apomonomer of enzymes.

The results presented in this paper demonstrate that *M. tuberculosis* contains two SHMTs, which despite having about 66% sequence homology have significantly different structural and stability properties. The most significant structural difference between SHM1 and SHMTs from various other sources including SHM2 is the presence of 1 mol of PLP/enzyme dimer in SHM1 as compared with 2 mol of PLP/enzyme dimer for all other reported SHMTs. Such a change in the stoichiometry of PLP and enzyme in SHMTs would have significant consequences in the structure and stability of SHM1 as PLP has been shown to play a significant role in functional activity and stability of SHMTs (15). Besides this, the SHM1 was found to have a lesser secondary structure and less compact conformation than the SHM2. Regarding the stability differences between the SHM1 and SHM2, it was observed that the SHM2 was more stable than SHM1 against thermal denaturation. However, SHM1 showed higher stability than SHM2 against alkaline denaturation.

Comparative analysis of mammalian SHMTs (12–14) as reported in literature and the *M. tuberculosis* SHMTs (both the SHM1 and SHM2) reported in this paper suggest that significant differences exist in their structural and functional properties between these enzymes. For example, the mammalian SHMTs are tetramers, whereas the *M. tuberculosis* SHMTs are dimers. The mammalian SHMT contains the eight-residue conserved sequence VTTTTHK(Pyr)T near the active site lysyl residue (Lys-229 as in eSHMT) that forms the internal aldime with pyridoxal phosphate. However, the *M. tuberculosis* SHMTs show significant changes in the conserved threonine sequence in the octapeptide (Fig. 3). These unique features of *Mycobacterium* SHMTs compared with the mammalian SHMTs can be exploited for designing drugs against *M. tuberculosis*.

Acknowledgment—Dr. C. M. Gupta is thanked for constant support provided during the studies.

REFERENCES

1. Schirch, V. (1982) *Adv. Enzymol. Relat. Areas Mol. Biol.* **53**, 83–112
2. Mc Neil, J., Bogner, A., and Perlman, R. (1996) *Genetics* **142**, 371–381
3. Shane, B. (1989) *Vit. Horm.* **45**, 263–335
4. Shostak, K., and Schirch, V. (1988) *Biochemistry* **27**, 8007–8017
5. Contestabile, R., Paiardini, A., Pascarella, S., di Salvo, M. L., D'Aguzzo, S., and Bossa, F. (2001) *Eur. J. Biochem.* **268**, 6508–6525
6. Appling, D. (1991) *FASEB J.* **5**, 2645–2651
7. Garrow, T., Brenner, A., Whitehead, M., Chen, X. N., Duncan, R., Korenberg, J., and Shane, B. (1993) *J. Biol. Chem.* **268**, 11910–11916
8. Besson, B., Neuberger, M., Rebeille, F., and Dounce, R. (1995) *Plant Physiol. Biochem.* **33**, 665–673
9. Sakamoto, M., Masuda, T., Yanagimoto, Y., Nakano, Y., Kitaoka, S., and Tanigawa, Y. (1996) *Z. Biosci. Biotech. Biochem.* **60**, 1914–1944
10. Capelluto, D. G. S., Hellmann, U., Cazzulo, J. J., and Cannata, J. J. B. (1999) *Mol. Biochem. Parasitol.* **98**, 187–201
11. Capelluto, D. G. S., Hellmann, U., Cazzulo, J. J., and Cannata, J. J. B. (2000) *Eur. J. Biochem.* **267**, 712–719
12. Renwick, S. B., Snell, K., and Baumann, U. (1998) *Structure* **6**, 1105–1116
13. Scarsdale, J. N., Kazanina, G., Radaev, S., and Schirch, V. (1999) *Biochemistry*

- 38, 8347–8358
14. Venkatesha, B., Udgaonkar, J. B., Rao, N. A., and Savithri, H. S. (1998) *Biochim. Biophys. Acta* **1384**, 141–152
15. Cai, K., Schirch, D., and Schirch, V. (1995) *J. Biol. Chem.* **270**, 19294–19299
16. Cai, K., and Schirch, V. (1996) *J. Biol. Chem.* **271**, 2987–2994
17. Bhatt, A. N., Prakash, K., Subramanya, H. S., and Bhakuni, V. (2002) *Biochemistry* **41**, 12115–12123
18. Laemmli, U. K. (1970) *Nature* **227**, 680–685
19. Cai, K., and Schirch, V. (1996) *J. Biol. Chem.* **271**, 27311–27320
20. Taylor, R. T., and Weisbach, H. (1965) *Anal. Biochem.* **13**, 80–84
21. Manohar, R., Ramesh, K. S., and Appaji Rao, N. (1982) *J. Biosci.* **4**, 31–50
22. Malkin, L. Z., and Greenberg, D. M. (1964) *Biochim. Biophys. Acta* **85**, 117–131
23. Schirch, V., Hopkins, S., Villar, E., and Angelaccio, S. (1985) *J. Bacteriology* **163**, 1–7
24. Andrews, P. (1965) *Biochem. J.* **96**, 569–606
25. Ulevitch, R. J., and Kallen, R. G. (1997) *Biochemistry* **16**, 5342–5349
26. Lakowicz, J. R. (1983) *Principles of Fluorescence Spectroscopy*, Plenum Press, New York
27. Angelaccio, S., Pascarella, S., Fattori, E., Bossa, F., Strong, W., and Schirch, V. (1992) *Biochemistry* **31**, 155–162
28. Schirch, L., and Jenkins, N. J. (1964) *J. Biol. Chem.* **238**, 3797–3800
29. Schirch, V., and Mason, M. (1962) *J. Biol. Chem.* **237**, 2578–2581
30. Prakash, K., Prajapati, S., Ahmad, A., Jain, S. K., and Bhakuni, V. (2002) *Protein Sci.* **11**, 46–57